

## EFFECT OF LOADING CONDITIONS AND INITIAL STATE ON THE SPALL FRACTURE OF AN EXPLOSIVE RDX-BASED COMPOUND

V. K. Golubev and A. P. Pogorelov

UDC 539.4

*Results from examination of the spall fracture of GTK-70 explosive compound under shock loading are reported. Specimens 20 and 30 mm thick were impacted by 1.0-mm-thick steel plates accelerated by an explosion to velocities of 180–370 m/sec. Calculations of the loading conditions and spall fracture of the specimens are performed in an elastoplastic formulation. An analysis of the data obtained yields a simple empirical relation among the maximum tensile stress in the spall plane, the stress gradient in the tensile pulse, and the maximum stress in the loading shock wave. Normalization of the specimens leads to a certain decrease in the fracture load.*

The dynamic fracture of explosive compounds has been the subject of relatively few studies. Some aspects of this problem were considered by Hoge [1], Seaman et al. [2], and Golubev et al. [3]. Hoge [1] obtained results on dynamic fracture of PETN and four HMX-based compounds under uniaxial tension conditions. Strain rates of up to  $3 \cdot 10^3 \text{ sec}^{-1}$  were attained using the Hopkinson split rod method. The strength of the materials studied increased by a factor of 5 or 6 compared to results of static tests, and, on this basis, it was suggested that the results obtained be used as the lower bound of the spall strength. Seaman et al. [2] studied the spall fracture of specimens of Propellant A compound impacted by a plate made of Lucite. Various stages of spall fracture of the compound (from intact specimens to complete fragmentation) were examined at impact velocities between 44 and 191 m/sec, which correspond to calculated impact stresses between 80 and 370 MPa. Golubev et al. [3] studied the effect of heating on the spall fracture of four RDX- and HMX-based explosive compounds. Heating to 150°C did not decrease the macroscopic-spall strength of the compounds. Moreover, heating of GTK-70 compound to this temperature even led to an abnormal increase in the spall strength, which is due to transition of this compound to a highly elastic state. The present investigation seeks to determine the influence of shock-loading conditions, which are varied by changing the impact velocity and specimen thickness, and the initial state of the specimen, which depends on the molding technology and subsequent thermal treatment, on the spall strength of the particular explosive compound.

The specimens of GTK-70 compound used in shock tests were of disks of diameter 120 mm and thickness  $h_t$  prepared by hot molding. In this RDX-based compound, the mass fraction of TNT as a plastifier is 20% and the mass fraction of collodion cotton as a binder is 10%. Part of the specimens thus prepared was subjected to normalization, i.e., exposure to elevated temperature for 30 days. Shock-wave loading of the specimens was performed by an impact of a steel plate 1.0 mm thick accelerated to the required velocity  $w_p$  by gliding detonation of a layer of TP-83 plastic explosive. This loading system was used in previous studies of the shock sensitivity of explosives (see [4]). The experiments were performed with complete preservation of all fragments of loaded specimens. The character and degree of fracture of the specimens were visually inspected and analyzed, and the mean thickness of the fragments of the first spall layer  $h_s$  was determined.

---

Institute of Experimental Physics, Sarov 607190. Translated from *Prikladnaya Mekhanika i Tekhnicheskaya Fizika*, Vol. 40, No. 5, pp. 18–22, September–October, 1999. Original article submitted March 2, 1998.

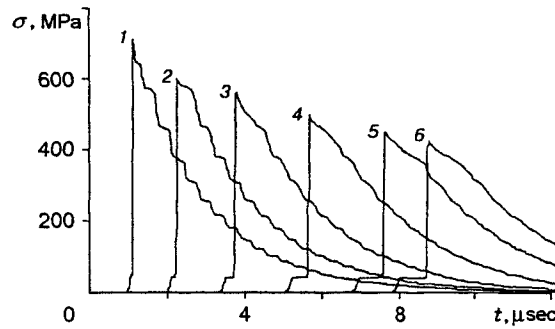


Fig. 1

TABLE 1

Material	$\rho_0$ , g/cm <sup>3</sup>	$c_0$ , km/sec	$n$	$\gamma$	$Y$ , MPa	$\nu$
Steel	7.85	4.63	4.21	1.70	750	0.28
GTK-70	1.72	2.37	7.38	1.20	20	0.34

For more accurate and complete determination of the fragments of the spall layer, a thin layer of a bright dye was applied on the rear surface of the specimens.

The conditions of shock-wave loading and spall fracture of the specimens were analyzed using a numerical calculation program for one-dimensional elastoplastic flows [5]. Primary attention was given to the Lagrangian coordinates corresponding to the sites of spall fracture. Complete diagrams of the longitudinal stress  $\sigma$  acting during the process of loading and unloading were plotted using these and similar coordinates. In a specimen layer 5 mm wide adjacent to the rear surface and in the region of the steel impactor, the density of the calculation grid cells was about 50 mm<sup>-1</sup>, and in the remaining volume of the explosive, it was 20 mm<sup>-1</sup>. In the calculations for the compound studied and for the impactor material (low-carbon St. 3 steel), the following Mie-Grüneisen equation of state was used:

$$P = \frac{\rho_0 c_0^2}{n} \left[ \left( \frac{\rho}{\rho_0} \right)^n - 1 \right] + \gamma \rho E_t.$$

Here  $P$  is the pressure,  $\rho$  is the density of the material,  $\rho_0$  is the initial density,  $c_0$  is the volumetric velocity of sound,  $\gamma$  is the Grüneisen parameter, and  $E_t$  is the specific thermal energy. The parameter  $n$  was chosen using data on the shock-wave compressibility of materials at relatively low pressures. The elastoplastic properties were taken into account by specifying the dynamic yield strength  $Y$  and the Poisson's coefficient  $\nu$ .

To elucidate the character of distribution of the loading pulse in the specimens, we performed experiments in which pulsed pressures at different distances from the collision surface were recorded. In all cases, the impact velocity was set equal to 170 m/sec, and manganin pressure gauges were placed at coordinates 3, 10, 20, and 23 mm. As a result, mechanical pulses with peak pressures of 560, 510, 460, and 410 MPa were recorded. In the calculations, the value of  $Y$  was varied to determine the effective dynamic yield strength of the compound studied. Figure 1 gives the calculated stress diagrams 1-6 at  $Y = 20$  MPa that correspond to the sections located at 3, 6, 10, 15, 20, and 23 mm from the impact surface. In this case, the best agreement between the experimental and calculated results was attained. Table 1 lists the chosen parameters of the equation of state and the elastoplastic properties of the impactor materials that were used in the calculations.

Results of the experiments and calculations of the spall-fracture conditions for the GTK-70 specimens are shown in Table 2. Here  $\sigma_t$  is the maximum tensile stress on the spall coordinate,  $\sigma_c$  is the maximum longitudinal stress in the specimen near the impact surface, and  $\Delta\sigma/\Delta x$  is the pressure gradient in the tensile pulse. The conditional value of the failure load ( $\sigma_t$ ) was assumed to depend to some extent on the parameters describing the intensity and rate of shock-wave loading ( $\sigma_c$  and  $\Delta\sigma/\Delta x$ ). Indeed, even a

TABLE 2

Initial state	$h_t$ , mm	$w_p$ , m/sec	$h_s$ , mm	$\sigma_c$ , MPa	$\sigma_t$ , MPa	$\Delta\sigma/\Delta x$ , MPa/mm	
Starting material	20	205	3.0	885	260	87	
		285	2.5	1293	302	121	
		300	2.5	1373	311	124	
		304	2.5	1391	314	126	
		360	2.0	1690	300	150	
	30	180	3.0	767	182	61	
		212	3.0	921	216	72	
		280	2.2	1266	214	97	
	Normalized material	20	186	2.3	796	195	85
			229	1.9	1006	203	107
250			1.6	1112	189	118	
296			1.5	1347	196	131	
325			1.3	1501	197	151	
368			1.0	1735	164	164	

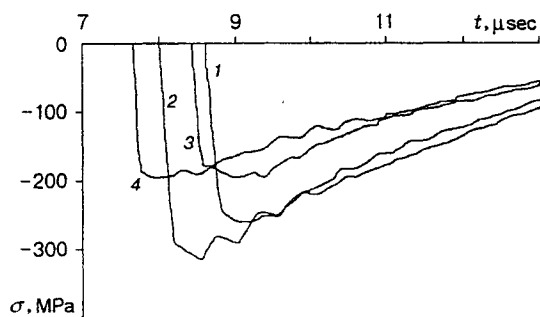


Fig. 2

preliminary examination of results of eight experiments with specimens of the starting material shows that  $\sigma_t$  increases somewhat with increase in the values of the chosen parameters. Figure 2 gives tensile stress curves for specimens 20 mm thick for both initial states and for greatly differing (by 100–110 m/sec) impact velocities (curves 1 and 2 correspond to the starting material and impact velocities 205 and 304 m/sec; curves 3 and 4 refer to the material subjected to normalization and impact velocities of 186 and 296 m/sec). Here it is necessary to note that normalization obviously decreases the failure load and smooths the tendencies exhibited by the starting material specimens.

In an additional experiment, a specimen of the starting material 40 mm thick was loaded by an impact of a steel plate 2.0 mm thick with a velocity of 80 m/sec. In this case, macroscopic spall fracture of the specimen was not detected. The calculated value of  $\sigma_c$  was 322 MPa, and the values of  $\sigma_t$  at 3, 6, 9, and 12 mm from the rear surface were 50, 84, 115, and 134 MPa, respectively.

In systematization of the results obtained, we first determined the minimum  $\sigma_{t,\min}$ , maximum  $\sigma_{t,\max}$ , and mean  $\bar{\sigma}_t$  failure loads for both initial states, and their standard deviations  $s$ . These results are given in Table 3 ( $N$  is the number of experiments performed for each of the initial states). Next, it was assumed that the dependence of the failure load on the parameters characterizing loading conditions is given by the following simple linear relation:

$$\sigma_t = a + b\Delta\sigma/\Delta x + c\sigma_c.$$

The multiple-regression parameters  $a$ ,  $b$ , and  $c$  and their standard deviations  $s_a$ ,  $s_b$ , and  $s_c$  obtained by

TABLE 3

Initial state	$N$	$\sigma_{t,\min} - \sigma_{t,\max}$ , MPa	$\bar{\sigma}_t$ , MPa	$s$ , MPa
Starting material	8	214–314	262.4	52.1
Normalized material	6	164–203	190.7	13.8

TABLE 4

Initial state	$R$	$s$	$F$	$a \pm s_a$ , MPa	$b \pm s_b$ , mm	$c \pm s_c$
Starting material	0.963	16.5	32.2	$142.2 \pm 25.4$	$3.85 \pm 0.77$	$-0.236 \pm 0.075$
Normalized material	0.732	12.1	1.74	$194.5 \pm 40.3$	$1.35 \pm 1.62$	$-0.139 \pm 0.137$

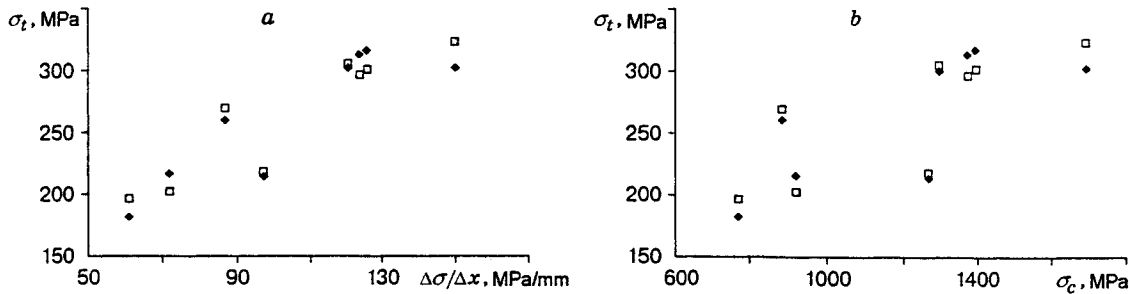


Fig. 3

regression analysis are given in Table 4 for both initial states. Here  $R$  is a correlation factor and  $F$  specifies the significance of regression. A comparison of the standard deviations  $s$  for the averaged (Table 3) and regression (Table 4) representations of the results obtained leads to the conclusion that the simple linear regression model is adequate for describing the spall-fracture conditions for specimens of the starting material. The applicability of this approach is illustrated in Fig. 3, which gives results of determination of the spall-fracture conditions for specimens of the starting material (filled points) and representations using the regression equation obtained (open points). Figure 3 a and b shows the dependences of the failure load  $\sigma_t$  on the tensile pulse pressure gradient  $\Delta\sigma/\Delta x$  and on the intensity of the loading shock wave  $\sigma_c$ , respectively. As regards results of spall fracture of the specimens subjected to normalization, since few experiments were performed and specimens of just one thicknesses were used, we were not able to determine the effect of loading conditions on the magnitude of failure load.

Let us discuss the results obtained. To estimate the decrease in the spall resistance due to normalization for the examined compound; we compare the mean values  $\bar{\sigma}_t$  obtained for specimens of the same thickness (20 mm) in an almost similar range of shock velocities. For the starting compound, this value is  $(297.4 \pm 21.7)$  MPa (5 experience), and, after normalization, it is  $(190.7 \pm 13.8)$  MPa (6 experiments). Thus, the decrease in the dynamic strength of the compound due to normalization is about 36%. In loading by an impact of maximum intensity (1.69–1.73 GPa), both initial states show a tendency toward a decrease in the calculated values of  $\sigma_t$ . This can be associated with the effect of additional energy release due to the decomposition reaction beginning in the explosive layer closest to the collision surface. In similar experiments, loading with an intensity of about 2.0 GPa leads to initiation of detonation in the examined compound. The results obtained in loading of a specimen that retained macroscopic integrity by an impact of a plate 2.0 mm thick with a velocity of 80 m/sec under a maximum tensile stress of 140 MPa agree well with the remaining results obtained and can serve as a reference bound of the resistance of the compound to shock loading. These results are close to the critical fracture level determined in [3] for 4 mm-thick GTK-70 specimens, which is characterized by a loading pulse pressure of 160–170 MPa. It can be assumed that the results obtained adequately describe the macroscopic spall-fracture conditions for the examined explosive compound.

We are grateful to Yu. V. Bat'kov for measuring pulsed pressure and B. L. Glushak for discussions of the experiments.

## REFERENCES

1. K. G. Hoge, "Dynamic tensile strength of explosive materials," *Explosivstoffe*, No. 2, 39–41 (1970).
2. L. Seaman, D. R. Curran, and W. J. Murri, "A continuum model for dynamic tensile microfracture and fragmentation," *Trans. ASME, Ser. E. J. Appl. Mech.*, **52**, No. 3, 593–600 (1985).
3. V. K. Golubev, S. A. Novikov, and Yu. S. Sobolev, "Effect of heating on the cleavage fracture of certain explosive compounds," *Fiz. Goreniya Vzryva*, **31**, No. 5, 129–131 (1995).
4. A. P. Pogorelov, B. L. Glushak, S. A. Novikov, and V. A. Sinitsyn, "Dependence of initiation pressure for 50/50 TNT/RDX on the pulse length in the collision of a thin steel plate," *Fiz. Goreniya Vzryva*, **13**, No. 2, 294–296 (1977).
5. N. F. Gavrilov, G. G. Ivanova, V. N. Selin, and V. N. Sofronov, "UPOK Program for solving problems of the mechanics of continuous media in the one-dimensional complex," *Vopr. Atom. Nauki Tekh., Ser. Metod. Progr. Chisl. Resh. Zadach Mat. Fiz.*, No. 3, 11–21 (1982).